be discussed further in the forthcoming article[11] already referred to, where the conclusions drawn here are examined in the light of evidence from other related experiments.

Because of the smallness of the parameter $(\lambda_1/\gamma\Delta^2)=\alpha$ our present data give only circumstantial evidence that Q has indeed the functional dependence expressed by Eq. (8). The experimental points (Fig. 2) could be connected by a straight line for either material. Measurements in considerably higher fields are needed to overcome this shortcoming, and we plan to carry these out in the near future. We also hope to perform quenching experiments in the presence of an rf field to measure γ more directly.

ACKNOWLEDGMENTS

It is a pleasure to acknowledge the patient and skillful contributions of K. H. Benford and R. B. Frank to the design and construction of the electronic circuitry used in this experiment. We are indebted to Dr. R. L. Garwin for occasional but illuminating suggestions on the same subject.

PHYSICAL REVIEW VOLUME 104, NUMBER 4 NOVEMBER 15, 1956

Distribution in the Upper Atmosphere of Sodium Atoms Excited by Sunlight*

T. M. DONAHUE, ROBERT RESNICK, AND V. ROBERT STULL
The University of Pittsburgh, Pittsburgh, Pennsylvania
(Received July 12, 1956)

Calculation is made of the distribution of atoms excited to the $^2P_{\frac{1}{2}}$ state by solar radiation, direct and reflected from the earth for a model sodium layer between 70 and 100 km. Account is taken of the attenuation by resonance absorption of sunlight in the layer before the solar photons reach a given point in the layer. This absorption grossly modifies the scattered intensity at twilight, causing minima to appear at about 5° solar depression and reducing greatly the difference in scattering for thicknesses between 2×10^9 cm^{-2} and 2×10^{11} atoms/cm^2 in late twilight. The effect of imprisonment, not included, is expected to modify only the late twilight results.

1. INTRODUCTION

IT is possible to explain the apparently great height of the sodium D line emission in the night air glow by taking account of the absorption of resonance radiation within the layer itself. Because of this absorption a layer below 100 km yields a zenith angle variation of intensity indistinguishable from that for a much higher layer without absorption. For this, however, it is required that the vertical thickness of sodium be not less than 1.5×10^{10} atoms/cm^2. Such a value for the thickness is so much in the extreme upper range of the numbers obtained from twilight scattering that careful attention to this method of obtaining the thickness is indicated. The method is simple.[1-4] The scattered intensity is taken to be

$$I_s=J_0\sigma\int_{r_1}^{r_2}Ndh, \qquad (1)$$

where J_0 is the incident solar flux at the bottom of the Fraunhofer line at the wavelength or on the wavelength range used. σ is the effective scattering cross section there. N is the density of sodium atoms as a function of the altitude h, and r_1 and r_2 are the limiting heights for the layer. Experimentally, I_s is obtained only after elaborate measures are taken to subtract the scattered intensity from the rest of the atmosphere.

Examination of the cases in which this method has been applied reveal that J_0 is taken to be the flux outside the atmosphere rather than at the scattering region. But to reach the scattering region at twilight the solar radiation must pass through a thickness of sodium which may be very large even when the vertical thickness is only 2×10^9 atoms/cm^2. The effect of the consequent attenuation on the scattering at the center of the D_2 component has been set forth in an earlier paper.[5] In brief, it was to reduce the scattered intensity for 2×10^{10} atoms/cm^2 over most of the post-sunset period to less than that for 2×10^9 atoms/cm^2 and to produce a decided minimum in the scattered intensity at about 3.5° solar depression. It became apparent that no simple interpretation of the scattering such as that offered on the basis of (1) was possible and that a careful study of the absorption and scattering taking into account the line shape and imprisonment of resonance radiation ought to be attempted. This papea presents the results of a calculation of the density of sodium atoms in the $^2P_{\frac{1}{2}}$ state excited directly by sunlight or by sunlight once reflected from the surface

* The work reported in this paper was supported in part by a grant from the National Science Foundation.
[1] D. R. Bates and H. S. W. Massey, Proc. Roy. Soc. (London) A187, 261 (1946).
[2] D. Barbier, Ann. Geophys. 4, 193 (1948).
[3] D. M. Hunten, J. Atmos. and Terrest. Phys. 5, 44 (1954).
[4] D. M. Hunten and G. G. Shepherd, J. Atmos. and Terrest. Phys. 5, 57 (1954).
[5] T. M. Donahue and R. Resnick, Phys. Rev. 98, 1622 (1955).

of the earth for sodium layers of several thicknesses between 2×10^9 atoms/cm^2 and 2×10^{11} atoms/cm^2 located between 70 and 100 km above the earth.

2. PATH OF INCIDENT SUNLIGHT

The sodium atoms are taken to be distributed according to

$$N(r)=N_0\exp[-\alpha(r-r_0)] \tag{2}$$

between r_1 and r_2. The thickness, L, of sodium traversed as in Fig. 1 by a solar photon which reaches a point (r,θ_0) in the layer has already been calculated for values of the impact parameter, p, larger than the earth radius.[5] These calculations were extended to smaller p and the thicknesses extrapolated to $p=0$ for three layers. These layers are described by

$$\begin{aligned} N(r)&=0, && r<6.47\\ &=N_0\exp[-127(r-6.40)], && 6.47<r<6.50\\ &=0, && r>6.50, \end{aligned} \tag{3}$$

where distances are measured in thousands of km. Three values of N_0, 2.17×10^7 cm^{-3}, 2.17×10^8 cm^{-3}, 2.17×10^9 cm^{-3} lead to layers of vertical thickness 2.31×10^9 cm^{-2}, 2.31×10^{10} cm^{-2}, and 2.31×10^{11} cm^{-2}, respectively. The actual path through the layer may traverse as many as 73 times the vertical number of atoms per cm^2 when p is 6.47×10^3 km and even as many as 12.2 times the vertical thickness when p is 6.40×10^3 km.

3. EXCITATION BY DIRECT SUNLIGHT

If the intensity per unit frequency incident on the earth's upper atmosphere at the bottom of the D_2 Fraunhofer line is taken to be J_0, independent of frequency, then the number of atoms excited to the $^2P_{\frac{3}{2}}$ state per second in a volume element $dV=drdA$ at (r,θ_0) will be

$$\omega_0'dV=J_0dA\int\exp[-\sigma(\nu)L]k(\nu)d\nu dr. \tag{4}$$

If the assumption is made now that the line is such that the absorption coefficient, $k(\nu)$, is everywhere proportional to the emission probability, $P(\nu)$, and the layer sufficiently homogeneous in line shape that the theory of imprisonment of resonance radiation may be applied, then the integral over the frequency spectrum in (4) is very closely related to

$$T(\sigma_0L)=\int P(\nu)\exp[-\sigma(\nu)L]d\nu, \tag{5}$$

where σ_0 is the absorption cross section at the center of the line. This function of σ_0L has been discussed by Holstein in connection with imprisonment of resonance radiation.[6,7] It is just the probability that a resonance photon will be emitted at a point in a gas and travel through a thickness L of absorbers without being absorbed. If it is assumed that

$$P(\nu)=ak(\nu), \tag{6}$$

then

$$T(\sigma_0L)=a\int k(\nu)\exp[-\sigma(\nu)L]d\nu, \tag{7}$$

and a is determined by the condition

$$P(\nu)d\nu=a\int k(\nu)d\nu=a\left(\frac{\lambda_0^2}{8\pi}\right)\left(\frac{g_2}{g_1}\right)\left(\frac{N}{\tau}\right), \tag{8}$$

where λ_0 is the wavelength at the center of the line g_2/g_1 the relative degeneracy of excited and ground state, τ the mean life of the excited state and N the density of absorbers at the point where the absorption is occurring. Thus

$$\int k(\nu)\exp[-\sigma(\nu)L]d\nu=\left(\frac{\lambda_0^2}{8\pi}\right)\left(\frac{g_2}{g_1}\right)\left(\frac{1}{\tau}\right)NT(\sigma_0L). \tag{9}$$

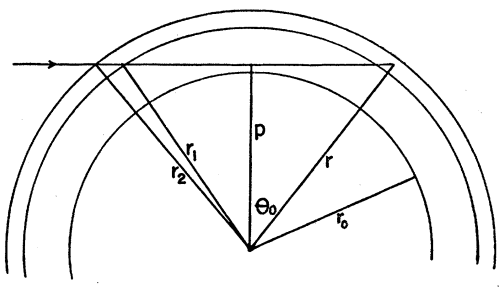

FIG. 1. Geometry of the direct transmission and absorption problem. The sun is to the left.

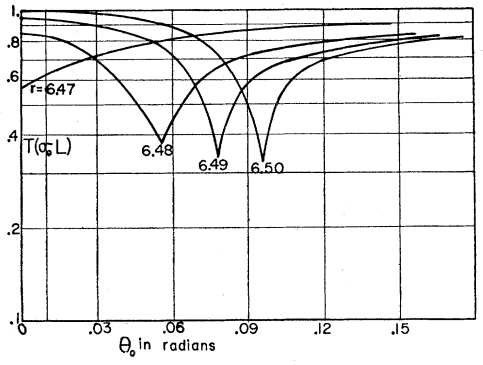

FIG. 2. Transmission function for resonance radiation arriving at angles of solar depression θ_0 for four altitudes in the layer. r is measured in thousands of km. Layer thickness: 2.31×10^9 atoms/cm^2.

[6] T. M. Donahue and A. Foderaro, J. Geophys. Research **60**, 75 (1955).
[7] T. Holstein, Phys. Rev. **72**, 1212 (1947); **83**, 1159 (1951).

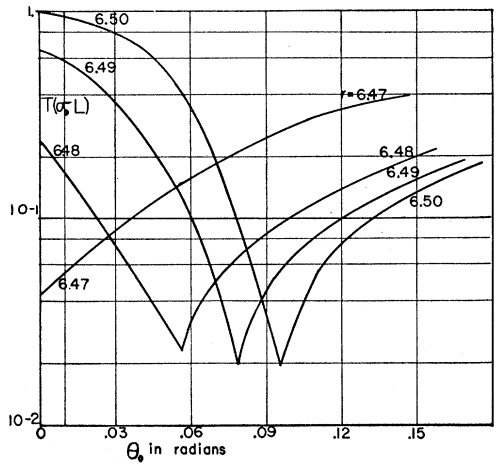

FIG. 3. Transmission function for layer 2.31×10^{10} atoms/cm² thick.

For a Doppler line shape, the cross section at the center of the line is

$$\sigma_0=\left(\frac{\lambda_0^3}{8\pi}\right)\left(\frac{g_2}{g_1}\right)\left(\frac{1}{\pi^{\frac{1}{2}}v_0\tau}\right), \tag{10}$$

where $v_0=(2RT/M)^{\frac{1}{2}}$. Therefore, the relationship between (5) and the integral over the frequency spectrum in (4) is

$$\int k(\nu)\exp[-\sigma(\nu)L]d\nu=(\pi^{\frac{1}{2}}v_0\sigma_0/\lambda_0)T(\sigma_0L)N. \tag{11}$$

The rate of excitation ω_0' at (r,θ_0) thus becomes

$$\omega_0'dV=[(\pi)^{\frac{1}{2}}v_0\sigma_0/\lambda_0]J_0T(\sigma_0L)N(r_0,\theta_0)dV. \tag{12}$$

$T(\sigma_0L)$ has been computed and tabulated as a function explicitly of σ_0L previously for the Doppler line shape assumed in this problem.[6] Since for every point (r,θ_0) in the layer, the thickness L of sodium traversed by the light is known from Sec. 2, and since the cross section σ_0 for the sodium D_2 line with a Doppler shape at 240° is 10^{-11} cm², it is possible to plot T as a function of θ_0 at various levels in the layer. This is done for three vertical thicknesses in Figs. 2, 3, and 4. Only values after sunset, $\theta_0=0$, are shown although the computation was carried out for all angles of solar depression back to noon ($\theta_0=-\pi/2$). The pronounced minima in the transmission function occur for points on the line with impact parameter $p=6.47\times10^3$ km. These curves are to a certain extent comparable with those for $\exp(-\sigma_0L)$ which have been published previously.[5] However, the function $T(\sigma_0L)$ not only takes into account the attenuation for all frequencies in the line, it contains the effect of the variation of absorption cross section as well. The result is a much weaker variation with θ_0 in this case. However, as will presently be apparent, the reduction is not sufficient to modify seriously the previously published conclusions based on attenuation at the center of the line.[5]

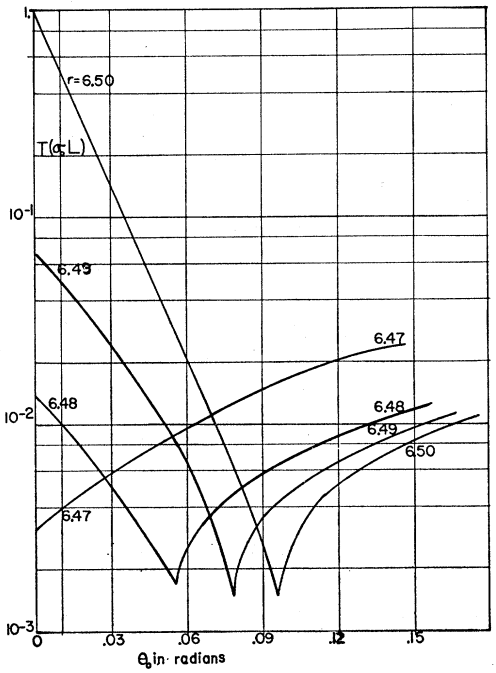

FIG. 4. Transmission function for layer 2.31×10^{11} atoms/cm² thick.

It might be mentioned also, concerning the spectrum of the radiation absorbed at a point in the twilight zone,

$$J_0\exp[-\sigma_0L]k(\nu)d\nu \text{ cm}^{-3}\text{ sec}^{-1}, \tag{13}$$

that it is apt to be severely "self-reversed" when $\sigma_0L\gg1$. This is not of any experimental consequence, however, since the radiation which is re-emitted and subsequently observed has simply the Doppler shape impressed by conditions at the point of emission.

If the transmission functions represented in Figs. 2, 3, and 4 are multiplied by the density of sodium atoms $N(r)$, they become proportional then to the rate at which sodium atoms are excited at (r,θ_0) by photons directly from the sun. To this rate must be added the effect of photons which traverse the layer, reflect from the earth's surface, and arrive at the point (r,θ_0) without previous absorption.

4. REFLECTION FROM THE EARTH

The geometry for the reflection problem is represented in Fig. 5. A typical photon path from the sun to the point (r,θ_0) in the layer is represented. In the system of coordinates used the point of reflection on the surface of the earth is identified by polar coordinates, r_0, η, β. The point in the layer receiving the radiation is on the polar axis of this coordinate system a distance r from the center of the earth. The plane perpendicular to the solar rays then makes an angle θ_0 with the $\beta=0$ plane.

Let an element of surface area on the earth be represented by $dA=r_0^2\sin\eta d\eta d\beta$. Then the number of

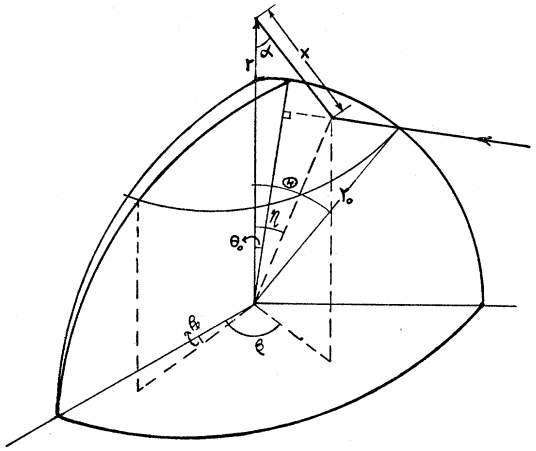

FIG. 5. Geometry of the reflection problem. The sun is to the right.

photons in the frequency range from ν to $\nu+d\nu$ striking dA after a passage through a thickness L, of sodium atoms will be

$$J_0 \exp[-\sigma(\nu)L_1]dA \cos\phi_1 d\nu, \tag{14}$$

where ϕ_1 is the angle between the normal to the surface and the incoming solar rays at the reflection point. Of these a fraction $g/2\pi$ will be reflected per unit solid angle, where g is the reflection probability. We take a Lambert's Law reflector for the surface of the earth. The fraction reflected into solid angle $d\Omega$ defined by the volume element dV at the point r on the polar axis is then

$$(g/2\pi)\cos\phi_2 d\Omega, \tag{15}$$

where $\phi_2=(\eta+\alpha)$ is the angle between the surface normal and the reflected ray. If the distance between the reflection point and the absorption point is called

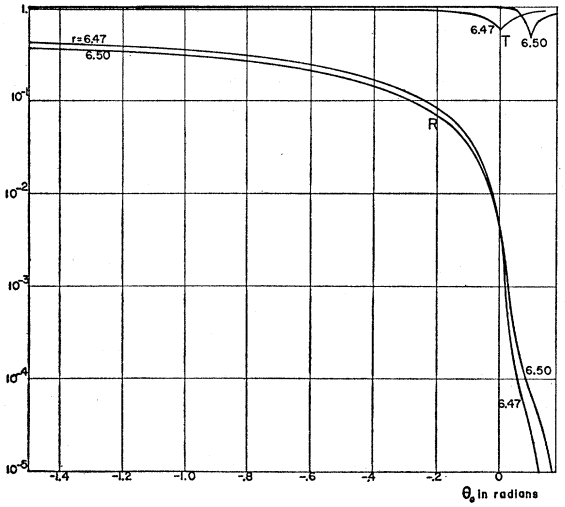

FIG. 6. Transmission and reflection functions at the top and the base of the layer. Layer thickness: 2.31×10^9 atoms/cm^2. $\theta_0=0$ corresponds to sunset. Heights, r, are in thousands of km.

x, then the number of photons absorbed per second in dV and in the frequency range $d\nu$ is

$$J_0 e^{-\sigma(\nu)L_1}dA \cos\phi_1 \frac{g}{2\pi}\cos\phi_2 e^{-\sigma(\nu)L_2}k(\nu)\frac{dV}{x^2}d\nu. \tag{16}$$

The rate of excitation by once reflected photons in dV is then obtained by an integration over the spectrum and over the area of surface visible at dA and illuminated by the sun. This is

$$\omega_0''=\frac{2g}{2\pi}J_0 r_0^2\int_{\beta_l}^{\pi/2}d\beta\int_{\theta_0}^{\Theta}\int k(\nu)e^{-\sigma(L_1+L_2)}d\nu \times\frac{\cos\phi_1\cos\phi_2}{x^2}\sin\eta d\eta. \tag{17}$$

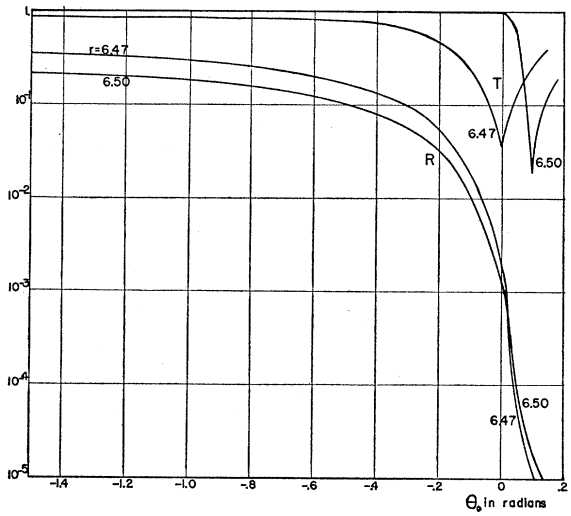

FIG. 7. Transmission and reflection functions for 2.31×10^{10} cm^{-2} layer.

Here β_l and Θ are limiting values set by the sunset arc and by the extreme ray which can reach dV from the earth's surface.

From our previous discussion it is clear that this integral involves $T(L_1+L_2)$, the transmission function for the sum of two thicknesses each of which depends on the location of the point of reflection.

$$\omega_0''dV=[\pi^{\frac{1}{2}}\sigma_0 v_0/\lambda_0]J_0\int_{\beta_l}^{\pi/2}d\beta\int\frac{g}{\pi}T(L_1+L_2) \times\frac{\cos\phi_1\cos\phi_2}{x^2}\sin\eta d\eta N dV. \tag{18}$$

In the Appendix it will be shown that it was possible to evaluate a very similar integral which contained an extra factor, $\cos\alpha$, in the integrand but not, of course, $T(L_1+L_2)$. This integral was multiplied by the mean

value of $T(L_1+L_2)\sec\alpha$ and the result called $R(\theta_0,r)$. In terms of this function,

$$\omega_0''dV=J_0(v_0\pi^{\frac{1}{2}}\sigma_0/\lambda_0)RNdV. \quad (19)$$

R has the same physical significance for the reflection problem as does the transmission function T of the direct excitation case. It is merely weighted with the requisite Lambert's law projection and reflection factors. With g, the reflection probability, taken as 0.5, R was obtained for all angles θ_0 from $-\pi/2$ to the end of twilight for the three thicknesses treated in this paper. In Figs. 6, 7, and 8 it is plotted at the top and bottom of the layer along with T, the counterpart of it in the direct excitation problem. In every case the decrease in effective surface area renders the reflected contribution negligible after sunset. During most of the day it is important, however, for all thicknesses, but particularly for the thinner layers where the chance

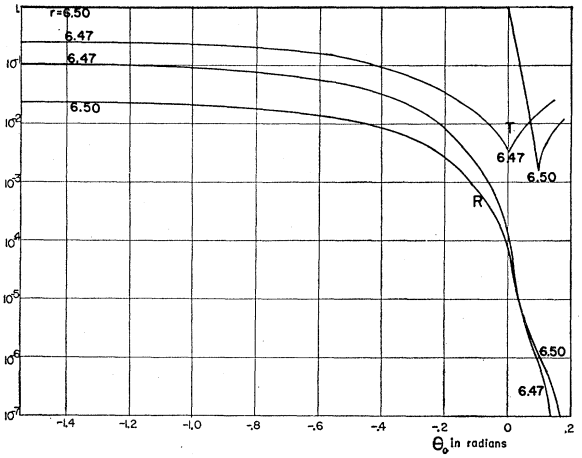

FIG. 8. Transmission and reflection functions for 2.31×10^{11} cm^{-2} layer.

that a photon should survive the initial traversal of the layer is better. Reflection is more important for the base of the layer because of the attenuation caused by longer passages of the layer except after sunset when the controlling factor is the area of the earth's surface visible.

5. PRIMARY DISTRIBUTION OF EXCITED ATOMS

The product of $(T+R)$ with the density of sodium atoms at every point as given by (3) yields finally a function proportional to the rate of creation of sodium atoms in the $^2P_{\frac{3}{2}}$ state by direct and once reflected solar radiation. Since this rate is just $n_0/J_0\tau$, where n_0 is the corresponding density of excited atoms and τ the mean life of the state, the final expression for the excitation distribution is

$$(n_0/\tau)dV=J_0(\pi^{\frac{1}{2}}v_0\sigma_0/\lambda_0)(T+R)NdV. \quad (20)$$

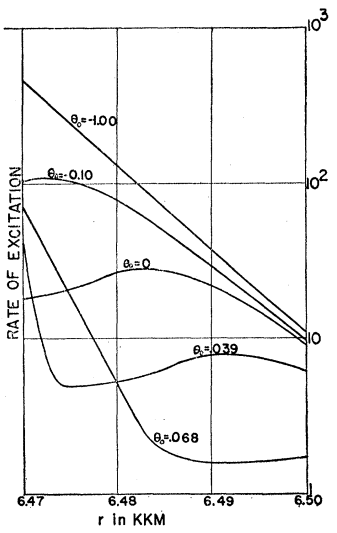

FIG. 9. Rate of excitation of sodium atoms to the $^2P_{\frac{3}{2}}$ state as a function of altitude at various angles of solar depression (radians). Layer thickness: 2.31×10^{10} atoms/cm^2. The unit on the vertical scale is 1 cm^{-1} sec in terms of atoms excited per unit volume per unit photon intensity per unit frequency.

Because there is no certain knowledge of J_0, a tabulation has been made of $n_0/J_0\tau$ and this is plotted as a function of r for selected θ_0 in the 2.31×10^{10} cm^{-2} and in the 2.31×10^{11} cm^{-2} layers in Figs. 9 and 10. The factor $\pi^{\frac{1}{2}}v_0\sigma_0/\lambda_0$ is 1.72×10^{-2} cm^2/sec, independent of T, and the unit of the vertical scale in these figures consequently is 1 sec cm^{-1}, representing a rate of excitation per unit volume per unit photon intensity per unit frequency interval. One very striking feature of these curves in the neighborhood of sunset is the fact that the attenuation of the light arriving in the lower reaches of the layer is so severe that it overpowers the exponential variation of sodium atoms. The consequence is that the primary excited atom population may actually rise with increasing altitude. In fact for the 2.31×10^{11} cm^{-2} layer the peak in the excited atom curve is near the top of the layer.

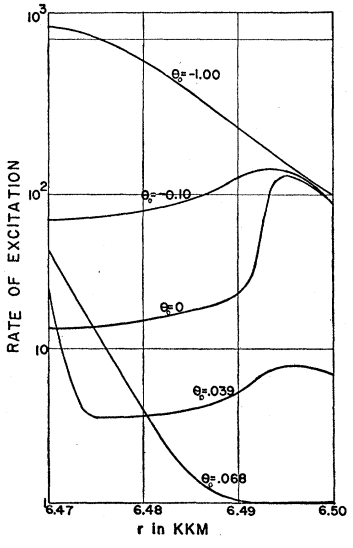

FIG. 10. Rate of excitation of sodium atoms to the $^2P_{\frac{3}{2}}$ state as a function of altitude for 2.31×10^{11} cm^{-2} layer. The vertical unit is 1 cm^{-1} sec.

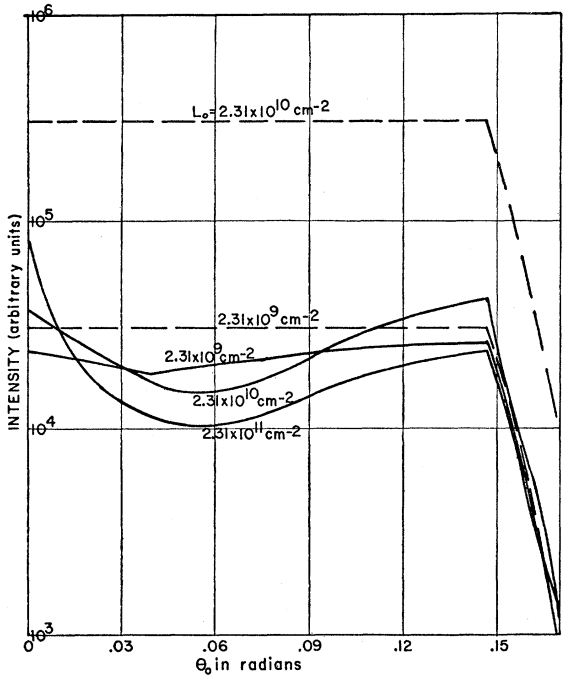

FIG. 11. Rate of excitation to the $^2P_{\frac{1}{2}}$ state per cm^2 column for three vertical thicknesses as functions of the angle of solar depression. The vertical unit is 10^3 sec in terms of transitions per cm^2 column per unit incoming intensity per unit frequency. The dashed lines give the scattered intensity predicted without attenuation.

6. SCATTERED INTENSITY

Integration of these curves along r gives the first approximation to the scattered intensity which should be observed for zenith observation. Curves for the three layers are plotted in Fig. 11 giving rate of radiation per cm^2 per unit photon intensity per unit frequency interval as functions of the angle of solar depression. These may be compared with the intensity variation which would be predicted if attenuation were neglected. It is notable that over this wide range of variation in layer thickness there results so little difference in the curves during the time when the lower border of sunlight is sweeping up through the layer. It is also interesting that the curves cluster about the unattenuated 2.31×10^9-cm^{-2} curve. The fundamental process which controls the phenomena contemplated here is of course the competition between the increasing scattering and the increasing attenuation as the layer grows thicker. The consequence is that during late twilight, just before intensity begins its decline, there is an optimum layer thickness in the neighborhood of 2.31×10^{10} atoms/cm^2. There is much less light to be observed from a 2.31×10^{11} cm^{-2} layer. The pronounced minimum near 0.05 radian solar depression is also notable. It is a consequence of the fact that at these angles the lower portion of the sodium layer is illuminated by radiation which has passed through a great thickness of sodium.

7. COMMENTS

These results will need to be modified by the contribution of imprisoned photons, those which are emitted by these excited atoms and produce in turn further excitation. However, this correction is expected to be important only for the very end of twilight, where only the top of the layer is accessible to primary photons and only for the thinner layers where great expanses of the sodium layer can make important contributions of secondary photons. It is possible, however, that the effect will be great enough near the end and *just after twilight* that the sodium layer may not have the geometry which the time of the end of the flash would seem to imply. An attempt is being made to determine whether the observations are actually compatible with a layer considerably below 100 km.

It should also be pointed out that when comparison is made between the light observed in the D lines and that detected in a nearby part of the spectrum for the purpose of subtracting the effect of lower-atmosphere scattering the scattering at the reference wavelength is not a fair index of the scattering at D-line wavelengths by the lower atmosphere. The sunlight scattered by the lower atmosphere must also traverse the sodium layer. A discussion of the effect of this phenomenon is being published elsewhere.

Finally, it seems that great care must be exercised in concluding anything about the density and distribution of atmospheric sodium from measurements on the twilight flash. Only detailed comparison of intensity variation which can be attributed unambiguously to the sodium layer with a theoretical calculation which accounts for resonance absorption and imprisonment together with all other such complicating factors as refraction and ozone attenuation can hope to yield reliable values for these quantities. It is by no means clear yet that from twilight data alone a layer as thick as 2×10^{11} sodium atoms per cm^2 column can be excluded.

8. APPENDIX

The coordinate system for this problem is shown in Fig. 5. In this system the circle on which the plane perpendicular to the sun's rays cuts the earth's surface is given by

$$\tan\eta \sin\beta = \tan\theta_0, \tag{21}$$

where θ_0 is the angle between this plane and the $\beta=0$ plane as measured for $\beta=\pi/2$. The problem, from (18), is to evaluate

$$\int_{\beta_1}^{\pi/2} \cos\phi_1 d\beta \int_{\theta_0}^{\Theta} \frac{[\cos\alpha]\cos(\eta+\alpha)}{x^2} \sin\eta d\eta, \tag{22}$$

where

$$\cos\phi_1 = \sin\eta \sin\beta \cos\theta_0 - \cos\eta \sin\theta_0 \tag{23}$$

determines the projection of the element of area in the direction of the sun. The term $[\cos\alpha]$ is not properly a

part of the integrand of (18), but only when it was included could the integration be carried through under certain conditions for θ_0. In such cases (22) must be multiplied by $\langle T(L_1+L_2)\sec\alpha\rangle_{Av}$.

The lower limit, β_l, of the azimuthal angle is set by the point at which the parallel of latitude defined by η intersects the great circle (21). There are three cases defined by the nature of β_l.

A. $0<\theta_0<\Theta$. This is the twilight case.
B. $-\Theta<\theta_0<0$. This is just before sunset.
In cases A and B, from (21),

$$\sin\beta_l=\tan\theta_0/\tan\eta. \tag{24}$$

C. $-\frac{1}{2}\pi<\theta_0<-\Theta<0$. In the daytime—back to noon—

$$\beta_l=-\pi/2.$$

Here the integral (22) can be evaluated without the extra term $[\cos\alpha]$.

In evaluating the integral (22), the integration over β is easily performed to give

$$\int_{\beta_l}^{\pi/2}(\sin\eta\sin\beta\cos\theta_0-\cos\eta\sin\theta_0)d\beta =(a^2-\mu^2)^{\frac{1}{2}}+c\mu(\beta_l-\pi/2), \tag{25}$$

where

$$a=\cos\theta_0,\quad c=\sin\theta_0,\quad\text{and}\quad \mu=\cos\eta. \tag{26}$$

The following relations can be seen from Fig. 5:

$$\begin{aligned} r_0^2&=x^2+r^2-2xr\cos\alpha,\\ r^2&=x^2+r_0^2+2xr_0\cos(\alpha+\eta),\\ x^2&=r^2+r_0^2-2rr_0\cos\eta. \end{aligned} \tag{27}$$

When (27) and (25) are appropriately substituted into (22), the result contains six terms, as follows:

$$\begin{aligned} &\frac{1}{4\pi r^2}\int_a^b(a^2-\mu^2)^{\frac{1}{2}}d\mu+\frac{c}{4br^2}\int_a^b\mu\beta_l d\mu-\frac{c\pi}{8br^2}\int_a^b\mu d\mu\\ &-\frac{(1-b^2)^2}{4br^2}\int_a^b\frac{(a^2-\mu^2)^{\frac{1}{2}}d\mu}{[(1+b^2)-2b\mu]^2}\\ &-\frac{(1-b^2)^2c}{4br^2}\int_a^b\frac{\mu\beta_l d\mu}{a[(1+b^2)-2b\mu]^2}\\ &+\frac{(1-b^2)\pi c}{8br^2}\int_a^b\frac{\mu d\mu}{[(1+b^2)-2b\mu]^2}, \end{aligned} \tag{28}$$

where

$$b=\cos\Theta \tag{29}$$

and, of course,

$$r=r_0/b. \tag{30}$$

All of these integrals are easily evaluated by the standard methods except for the second last which can be neglected on the grounds that its maximum value for typical values of r and θ_0 is about 0.05% of the value of the other five terms for case A and is about 5% of this for case B.

In case C the integral (22) without $[\cos\alpha]$ becomes

$$\int_{-\pi/2}^{\pi/2}\cos\phi_1 d\beta\int_0^{\Theta}\frac{\cos(\alpha+\eta)}{x^2}\sin\eta d\eta, \tag{31}$$

which can be evaluated exactly. For, use of the result that

$$\int_{-\pi/2}^{\pi/2}(\sin\eta\sin\beta\cos\theta_0-\cos\eta\sin\theta_0)d\beta=-\pi\sin\theta_0\cos\eta, \tag{32}$$

and (27), allows (31) to be written

$$\frac{\pi c}{r^2}\left\{\int_1^b\frac{\mu^2 d\mu}{(1+b^2-2b\mu)^{\frac{3}{2}}}-\int_1^b\frac{\mu d\mu}{(1+b^2-2b\mu)^{\frac{3}{2}}}\right\}, \tag{33}$$

which is easily seen to be

$$\frac{2\pi c}{3b^3r^2}\{(2+b^2)(1-b^2)^{\frac{1}{2}}-(2+b^3)=A. \tag{34}$$

The value of $R(\theta_0,r)$ is found as follows. For cases A and B,

$$R(\theta_0,r)=\frac{gr_0^2}{2\pi}\langle T(L_1+L_2)\sec\alpha\rangle_{Av}A', \tag{35}$$

where A' is given by the appropriate value of (28). For case C,

$$R(\theta_0,r)=\frac{gr_0^2}{2\pi}\langle T(L_1+L_2)\rangle_{Av}A, \tag{36}$$

where A is given in (34). Fortunately, the averaging processes for $T\sec\alpha$ could be carried out without much difficulty in most cases since these functions and the integrand of (22) varied slowly over the region of integration. Confidence in our averaging procedure was afforded by the fact that the curves drawn from (37) joined smoothly with those for the more exact expression (38). The results are shown graphically in Figs. 6, 7, and 8.